Chemistry
A European
Journal

Chemistry Europe
European Chemical Societies Publishing

Accepted Article

Title: Chlorophyll based organic heterojunction on Ti3C2Tx MXenes nano-sheets for efficient hydrogen production

Authors: Yuanlin Li, Yuliang Sun, Tianfang Zheng, Yohan Dall'Agnese, Chunxiang Dall'Agnese, Xing Meng, Shin-ichi Sasaki, Hitoshi Tamiaki, and Xiao-Feng Wang

To be cited as: *Chem. Eur. J.* 10.1002/chem.202005421

Link to VoR: https://doi.org/10.1002/chem.202005421

WILEY-VCH

10.1002/chem.202005421

Chlorophyll based organic heterojunction on $Ti_3C_2T_x$ MXenes nano-sheets for efficient hydrogen production

Yuanlin Li,[a, b] Yuliang Sun,[a, b] Tianfang Zheng,[a, b] Yohan Dall'Agnese,[c] Chunxiang Dall'Agnese,[a] Xing Meng,*[a, b] Shin-ichi Sasaki,[d, e] Hitoshi Tamiaki[d] and Xiao-Feng Wang*[a, b]

[a] Dr. Y. Li, Y. Sun, T. Zheng, C. Dall'Agnese, Prof. X. Meng, X.-F. Wang, Key Laboratory of Physics and Technology for Advanced Batteries (Ministry of Education), College of Physics, Jilin University, Changchun 130012, PR China

[b] Dr. Y. Li, Y. Sun, T. Zheng, C. Dall'Agnese, Prof. X. Meng, X.-F. Wang, Key Jilin Key Engineering Laboratory of New Energy Materials and Technologies, Jilin University, Changchun 130012, P. R. China

[c] Prof. Y. Dall'Agnese, Institute for Materials Discovery, University College London, London WC1E 7JE, United Kingdom

[d] Prof. S. Sasaki, Prof. H. Tamiaki, Graduate School of Life Sciences, Ritsumeikan University, Kusatsu, Shiga 525-8577, Japan

[e] Prof. S. Sasaki, Nagahama Institute of Bio-Science and Technology, Nagahama, Shiga 526-0829, Japan

*E-mail: mengxing@jlu.edu.cn (Xing Meng), xf_wang@jlu.edu.cn (Xiao-Feng Wang).

Abstract

Z-scheme process is a photo-induced electron transfer pathway in natural oxygenic photosynthesis involving the electron transport from photosystem II (PSII) to PSI. Inspired by the interesting Z-scheme process, here we demonstrated a photocatalytic hydrogen evolution reaction (HER) employing chlorophyll derivatives, Chl-1 and Chl-2, on the surface of $Ti_3C_2T_x$ MXenes with two-dimensional accordion-like morphology forming Chl-1@Chl-2@$Ti_3C_2T_x$ composite. Due to the frontier molecular orbital energy alignments of Chl-1 and Chl-2, the sublayer Chl-1 is a simulation of PSI whereas the upper layer Chl-2 is equivalent to PSII, and the resultant electron transport can take place from Chl-2 to Chl-1. Under the illumination of visible light (> 420 nm), the HER performance of Chl-1@Chl-2@$Ti_3C_2T_x$ photocatalysts was found to be as high as 143 μmol/h/g_{cat}, which was substantially higher than that of photocatalysts of either Chl-1@$Ti_3C_2T_x$ (20 μmol/h/g) or Chl-2@$Ti_3C_2T_x$ (15 μmol/h/g).

Introduction

Energy shortage will become a serious problem in the near future with the global economy growth requiring increasing consumption of energy.[1-3] Solar energy is a kind of abundant and clean energy, nearly four million exajoules (4×10^{18} J) of solar energy reaches the earth annually, which has the potential to meet the global demand of energy consumption.[2, 4, 5] Photocatalytic water splitting for hydrogen evolution is one of the sustainable approaches to convert solar energy into chemical energy. However, the traditional semiconductor photocatalytic hydrogen production systems are moderately

efficient and high-cost.[6]

Natural photosynthesis has evolved for billions of years, which converts solar energy into chemical energy based on their light-harvesting antenna and charge-separating reaction center systems. In recent years, photocatalytic fuel production systems were inspired by natural Z-scheme in oxygenic photosynthesis. The artificial systems have been studied by combining half-reactions to produce H_2 and O_2 through photocatalytic decomposition of water. The photosynthesis model system using dual semiconductors was introduced for water splitting in 1979.[7] The Z-scheme is the two-step photo-induced charge separation from photosystem II (PSII) to PSI through an electron transfer chain. This potential Z-scheme of particular concern in photo-induced electron transport chain processes enlightened us to design dual photoexcitation-based photocatalysts. As one of the most abundant natural photosynthetic pigments on the earth, chlorophylls (Chls) were selected to convert solar energy into chemical energy based on absorbing sunlight and transferring absorbed energy, due to the delocalization of their excited electrons around the π-conjugated tetrapyrrole ring.[8-10] The remarkable properties of charge transfer ability of Chls have been reported previously. It was shown that they can form aggregates to efficiently capture sunlight and transport charge compared with their monomers. Such properties of Chl derivatives have been applied in solar cells,[11-13] energy storage,[14] and photocatalytic hydrogen evolution.[15] Compared with other photocatalysts using synthetic photoactive materials, Chls are cost-effective, environmentally friendly, easy to dispose, abundant, and nonpoisonous natural pigments. Therefore, introduction of Chls in the hydrogen evolution reaction (HER) systems must

be of great potential.

Catalytic systems usually use noble metals as cocatalysts, such as Pt, Ru, Rh, and Pd, which increased the cost of catalytic systems, therefore limiting the commercialization for a large scale. MXenes, as a new family of two-dimensional (2D) nanostructured materials originally reported in 2011, are currently being widely studied for a wide variety of applications such as energy storage,[16-18] photoelectric materials,[19, 20] electromagnetic interference shielding,[21, 22] water purification,[23] and catalysis,[24] due to their outstanding physicochemical properties.[25] MXenes are prepared from MAX phases by etching an A layer (usually Al or Si) with a strong acid solution such as HF or LiF/HCl.[26] The general formula of MXenes is $M_{n+1}X_nT_x$ (n = 1-3), where M represents an early transition metal such as Ti, V, Nb, Ta, or Mo, X is C and/or N, and T_x represents a surface terminating group such as -O, -F and -OH.[18, 27, 28] It is worth noting that using $Ti_3C_2T_x$ MXenes as a co-catalyst presents remarkable advantages, such as good hydrophilicity, excellent metallic conductivity, good stability in aqueous solutions, and low cost.[29] Considering the above-mentioned excellent characteristics of $Ti_3C_2T_x$, it has become a very promising co-catalyst material in photocatalysis for HER.[30-32]

In our previous investigation, we combined zinc methyl 3-devinyl-3-hydroxymethyl-pyropheophorbide *a* (Chl-1) with $Ti_3C_2T_x$ MXene for HER, and we proved that hydrogen generated through the exciton transfer in Chl-1 aggregates followed by charge transfer to $Ti_3C_2T_x$.[15] However, the performance of this system was still insufficient and requires further improvement. In this work, we employ two Chls with different physical characteristics, i.e., Chl-1 acts as a PSI simulator for accepting electrons and methyl 13^1-

deoxo-13[1]-dicyanomethylene-pyropheophorbide *a* (Chl-2) acts as a PSII simulator for donating electrons. These Chls are deposited on $Ti_3C_2T_x$ MXenes co-catalyst to form noble metal-free Chl-based organic heterojunction photocatalyst for HER. The photocatalytic performance of Chl-1@Chl-2@$Ti_3C_2T_x$ photocatalyst exhibited a much higher hydrogen production than that of either Chl-1@$Ti_3C_2T_x$ photocatalyst or Chl-2@$Ti_3C_2T_x$ photocatalyst. To understand this performance improvement, measurements of electrochemical impedance spectroscopy (EIS) and transient photocurrent (TPC) responses were used to characterize these photocatalysts.

Results and discussion

Figure 1 shows the chemical structures of Chl-1 and Chl-2 used in the organic heterojunction photocatalysts. Their molecular structures are partially different on the C3- and C13-substituents of the chlorin macrocycle. Chl-1 has a hydroxymethyl group at the C3-position and a carbonyl group at the C13-position, whereas Chl-2 has a vinyl group at the 3-position and two cyano groups at the terminal of the 13[1]-methylene moiety. In addition, Chl-1 has a central zinc ion in its tetrapyrrole ring, while Chl-2 is a free base. It is worth mentioning that the 3[1]-hydroxy group, central metal zinc ion, and 13-carbonyl group along the molecular y-axis are of great significance for the self-assembly of Chl-1 to form *J*-aggregates.[33, 34] This is due to the coordination of the oxygen atom in the 3[1]-hydroxy group with the central zinc ion, and the formation of hydrogen bonds between the 3[1]-hydroxy and the 13-carbonyl groups, thereby forming a strong intermolecular interaction of Zn···O–H···O=C.[33, 35]

10.1002/chem.202005421

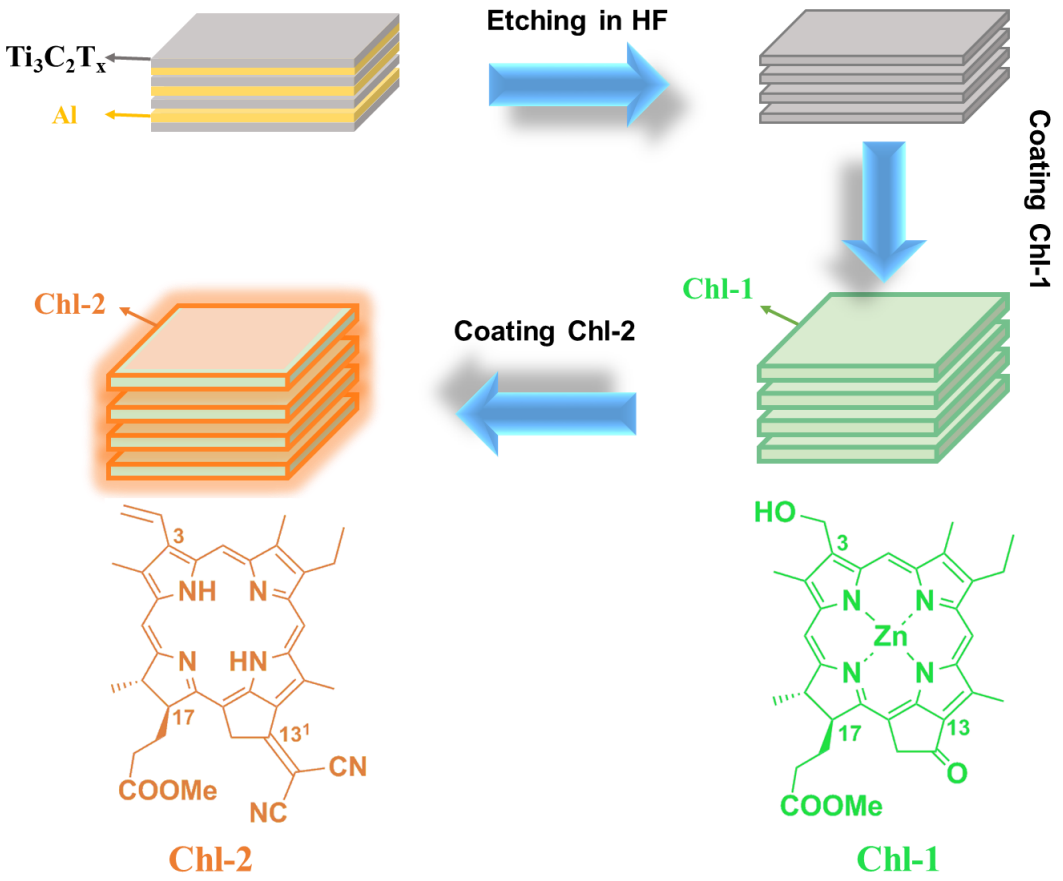

Fig. 1 Schematic diagram of the preparation process of Chl-1@Chl-2@$Ti_3C_2T_x$ composites (upper) and molecular structures of the two Chl derivatives (lower).

Figure 2a shows the X-ray diffractometer (XRD) patterns of the raw materials and the Chl-1@Chl-2@$Ti_3C_2T_x$ composites. The (002) and (004) peaks of Ti_3AlC_2 move toward low angles in $Ti_3C_2T_x$ and the strongest MAX phase peak at 39.0° disappeared, indicating that the Al layer was removed from Ti_3AlC_2. The XRD pattern of Chl-1 showed three typical peaks at 6.2°, 13.9°, and 25.2°, and Chl-2 showed three typical peaks at 5.6°, 9.0°, and 25.6°. The XRD pattern of the Chl-1@Chl-2@$Ti_3C_2T_x$ photocatalyst only showed the characters of $Ti_3C_2T_x$, and there were no typical peaks of Chl-1 and Chl-2. This is mainly due to the low mass ratio of Chls. The XRD patterns of the Chl-1@$Ti_3C_2T_x$

10.1002/chem.202005421

and Chl-2@$Ti_3C_2T_x$ photocatalyst also only showed the characters of $Ti_3C_2T_x$ (Fig. S1 in Supporting Information).

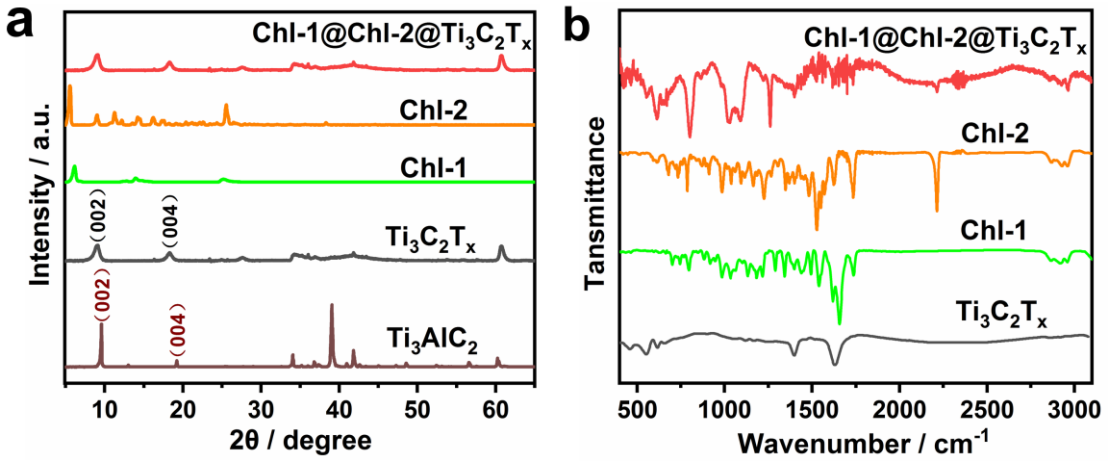

Fig. 2 (a) XRD patterns and (b) FT-IR spectra of the raw materials and the composites.

Figures 2b and S2 in SI show the Fourier transform infrared spectroscopy (FT-IR) spectra of these raw materials and composites. As previously reported, the two signals at 1390 and 1650 cm^{-1} could be attributed to O–H and C=O on $Ti_3C_2T_x$.[36] The small peaks between 2750 and 3000 cm^{-1} belong to the C–H in -CH_2 and -CH_3 of Chl-1 and Chl-2. Meanwhile, the peaks from 2200 to 2250 cm^{-1} can be attributed to C≡N and C≡C. The FT-IR spectra of Chl-1@Chl-2@$Ti_3C_2T_x$ photocatalyst is nearly identical to that of pure Chl-1, Chl-2 and $Ti_3C_2T_x$, indicating that formation of the composites are not through chemical bonding but physically combined.

Figure 3 shows the morphology of the $Ti_3C_2T_x$, Chl-1, Chl-2, and the composites by Scanning electron microscopy (SEM). As shown in Fig. 3a, a typical 2D nanosheet accordion-like structure could be clearly observed in the HF-etched $Ti_3C_2T_x$. In Figs. 3b and 3c, it could be seen that Chl-1 and Chl-2 were 2D materials with a layered structure.

10.1002/chem.202005421

Only the typical 2D nanosheet stack structure of $Ti_3C_2T_x$ was observed in Chl-1@Chl-2@$Ti_3C_2T_x$ photocatalysts, and no other significant changes are observed, as shown in Fig. 3d. Figure S3 show the SEM morphological images of the Chl-1@$Ti_3C_2T_x$, and Chl-2@$Ti_3C_2T_x$, respectively. One can easily observe the typical 2D nanosheet stack structure of $Ti_3C_2T_x$. The TEM images of Chl-1@Chl-2@$Ti_3C_2T_x$ composites are shown in Figs. 3e and 3f. Only the layered structure of $Ti_3C_2T_x$ could be observed, and Chl-1 and Chl-2 could not be observed. $Ti_3C_2T_x$ was identifiable in the high-resolution transmission electron microscopy (HRTEM) image by their corresponding crystal plane distances of 0.26 nm.

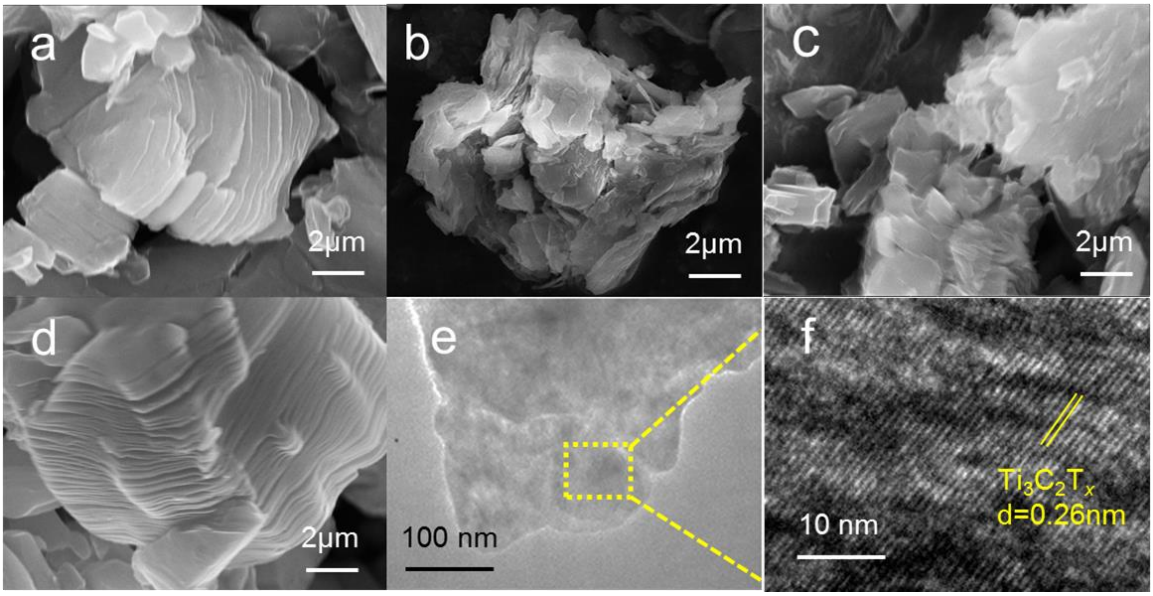

Fig. 3 SEM images of (a) $Ti_3C_2T_x$, (b) Chl-1, (c) Chl-2, (d) Chl-1@Chl-2@ $Ti_3C_2T_x$. (e) TEM and (f) HRTEM images of Chl-1@Chl-2@ $Ti_3C_2T_x$.

Figure 4 displays the electronic absorption spectra of the raw and composites materials. As previously reported, $Ti_3C_2T_x$ had no significant absorption peak due to its metallic properties.[37] In the cases of Chls, however, their absorption spectra show

significant red shifts after deposition on $Ti_3C_2T_x$, i.e., the Q_y bands shift from 647 nm in THF to 749 nm for Chl-1 and from 705 nm in THF to 752 nm for Chl-2: Chl absorption in THF can be found in Fig. S4 in Supporting Information. The red shifts in their absorption spectra are ascribable to the formation of *J*-aggregates. Thus, the absorption spectrum of the Chl-1@Chl-2@$Ti_3C_2T_x$ shows clearly mixed characteristics from respective Chl aggregates rather than from respective Chl monomers, suggesting that these Chls remain structural intact in the bilayer structure. The "pure" *J*-aggregates formed by π-π stacking of respective Chl-1 and Chl-2 molecules would facilitate the exciton delocalization in each Chl layer.[38]

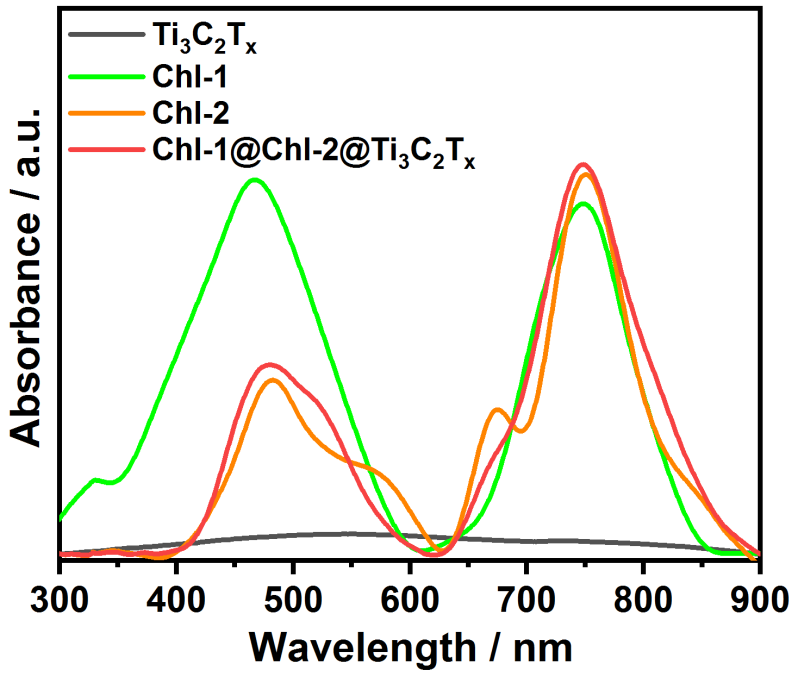

Fig. 4 Electronic absorption spectra of the three raw materials and the composites.

The HER performances of Chl-1@$Ti_3C_2T_x$, Chl-2@$Ti_3C_2T_x$, and Chl-1@Chl-2@$Ti_3C_2T_x$ photocatalysts as well as Chl-1+Chl-2+$Ti_3C_2T_x$ mixture (Chl-1, Chl-2, and $Ti_3C_2T_x$ were together dissolved in THF and stirred at room temperature for 10 h until dry)

10.1002/chem.202005421

are shown in Fig. 5. The best performance achieved was as high as 143 μmol/h/g_{cat} for the Chl-1@Chl-2@$Ti_3C_2T_x$ photocatalysts, which was higher than those of Chl-1@$Ti_3C_2T_x$ (20 μmol/h/g) and Chl-2@$Ti_3C_2T_x$ photocatalysts (15 μmol/h/g). The HER performance of Chl-1, Chl-2, and $Ti_3C_2T_x$ mixture (Chl-1+Chl-2+$Ti_3C_2T_x$) was also measured, but the performance was poor (14 μmol/h/g_{cat}). The mass ratio optimization in Chl-1@$Ti_3C_2T_x$, Chl-2@$Ti_3C_2T_x$ and Chl-1@Chl-2@$Ti_3C_2T_x$ photocatalysts were obtained (see Fig. S5).

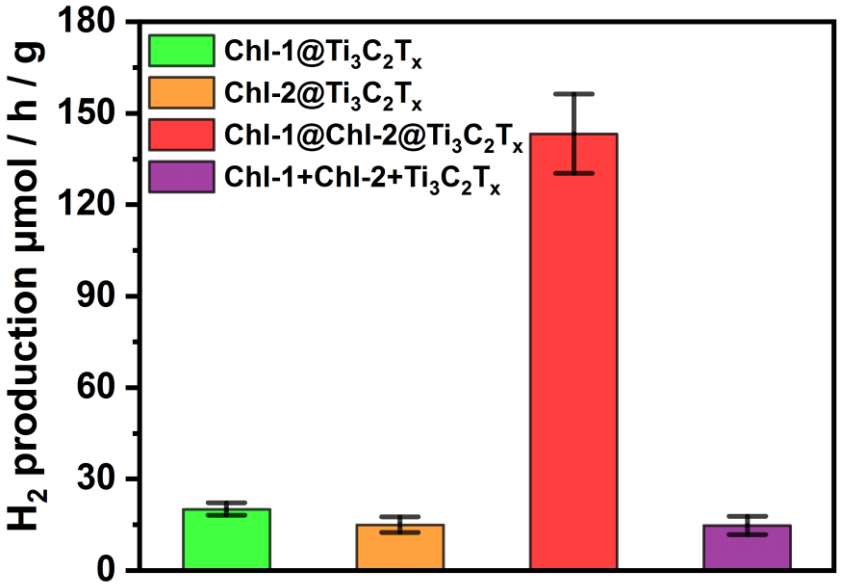

Fig. 5 Hydrogen production of Chl-1@$Ti_3C_2T_x$, Chl-2@$Ti_3C_2T_x$, Chl-1@Chl-2@$Ti_3C_2T_x$, and Chl-1+Chl-2+$Ti_3C_2T_x$.

EIS and TPC responses are shown in Fig. 6 to further study the improvement of carrier separation efficiency. The EIS Nyquist plot could be fitted to the equivalent circuit shown in Fig. 6a (inset), where R_1 is the electrolyte solution resistance and R_2 is the interface charge transfer resistance between electrode and electrolyte, while CPE and W_0 are the constant phase element and the Warburg impedance, respectively.[39] As shown in

10.1002/chem.202005421

Fig. 6a, the radius of the semi-circle of the Chl-1@Chl-2@$Ti_3C_2T_x$ photocatalysts was much smaller than those of the others, indicating a lower electron transfer resistance on the electrode surface and more efficient separation of photoelectron-hole pairs. Based on the fitting model, the fitted data for the samples were summarized in Table S1, in which the R_2 value of the Chl-1@Chl-2@$Ti_3C_2T_x$ photocatalysts was the smallest among these samples, indicating a high electron-hole pair separation efficiency.

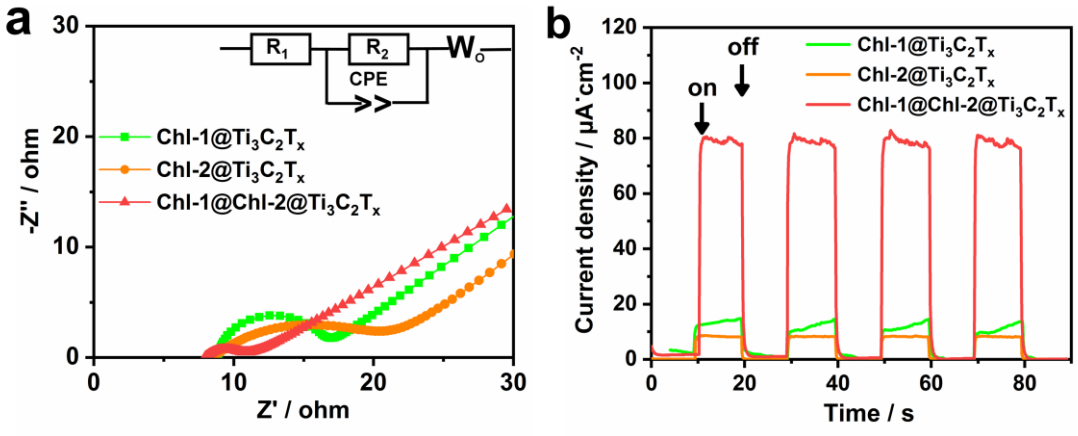

Fig. 6 (a) EIS Nyquist plots and (b) TPC responses of the hybrids.

TPC curves of different samples are shown in Fig. 6b. It could be seen that all samples showed an immediate rise of TPC response under illumination. Chl-1@Chl-2@$Ti_3C_2T_x$ photocatalysts showed a much higher photocurrent than those of the other composites, indicating Chl-1@Chl-2@$Ti_3C_2T_x$ photocatalysts could achieve higher photogenerated carrier separation and transfer efficiency. It was confirmed that the Chl-1@Chl-2@$Ti_3C_2T_x$ photocatalysts had an optimal charge transfer rate compared with the other composites, which explained its improved photocatalytic activity. The result of EIS and TPC response demonstrated that the Chl-1@Chl-2@$Ti_3C_2T_x$ photocatalysts have a larger potential than those single Chl-based composites, because the characteristics of the

suppression of electron-hole recombination, the improvement of carrier separation, and the reduction of transfer resistance of photogenerated holes and electrons are all essential for a highly efficient photocatalytic HER performance.

In natural photosynthesis, the so-called Z-scheme is the two-step photo-induced charge separation in PSII and PSI and an electron chain between the two photosystems (Fig. 7a).[40-42] First, upon four photons absorption by PSII, electrons are generated from the charge separation step in PSII, and two water molecules are split into four protons with the generation of one oxygen molecule. Second, the excited electrons are then transferred to photo-induced holes of PSI through an electron transport chain. Finally, the excited electrons gains sufficient potential energy (–0.58 V vs NHE, pH = 7) to reduce the nicotinamide adenine dinucleotide phosphate ($NADP^+$).[43] As a comparison, Figure 7b shows a hypothetical schematic diagram of the Chl-1@Chl-2@$Ti_3C_2T_x$ heterostructure for HER. Given that the HOMO and LUMO energy levels of Chl-1 are higher than those of Chl-2, respectively, Chl-1 functions similarly as P700 in PSI for accepting electrons and meanwhile Chl-2 mimics P680 in PSII for donating electrons. After the photo-excitation of Chl-1@Chl-2@$Ti_3C_2T_x$ composites by irradiation of visible-to-near infrared light ($\lambda > 420$ nm), Chl-1 are excited from the ground state to the excited state. Then, the electrons of the excited state of Chl-1 can be transferred to co-catalyst $Ti_3C_2T_x$ MXenes. Consequently, the electrons on $Ti_3C_2T_x$ MXenes combine with H^+ in aqueous ascorbic acid (AA) solution to generate hydrogen molecule. Meanwhile, the remaining hole of Chl-1 accepts an electron from Chl-2 of the excited state to reproduce Chl-1. This special

10.1002/chem.202005421

electron transport pathway enlarges the charge separated states of electrons and holes to improve the separation of electron-hole pair efficiency and suppressed their recombination simultaneously, resulting in a better photocatalytic hydrogen evolution activity. Besides, the holes of Chl-2 are reduced by the electron donor of AA, so that the photocatalyst Chl is completely regenerated.

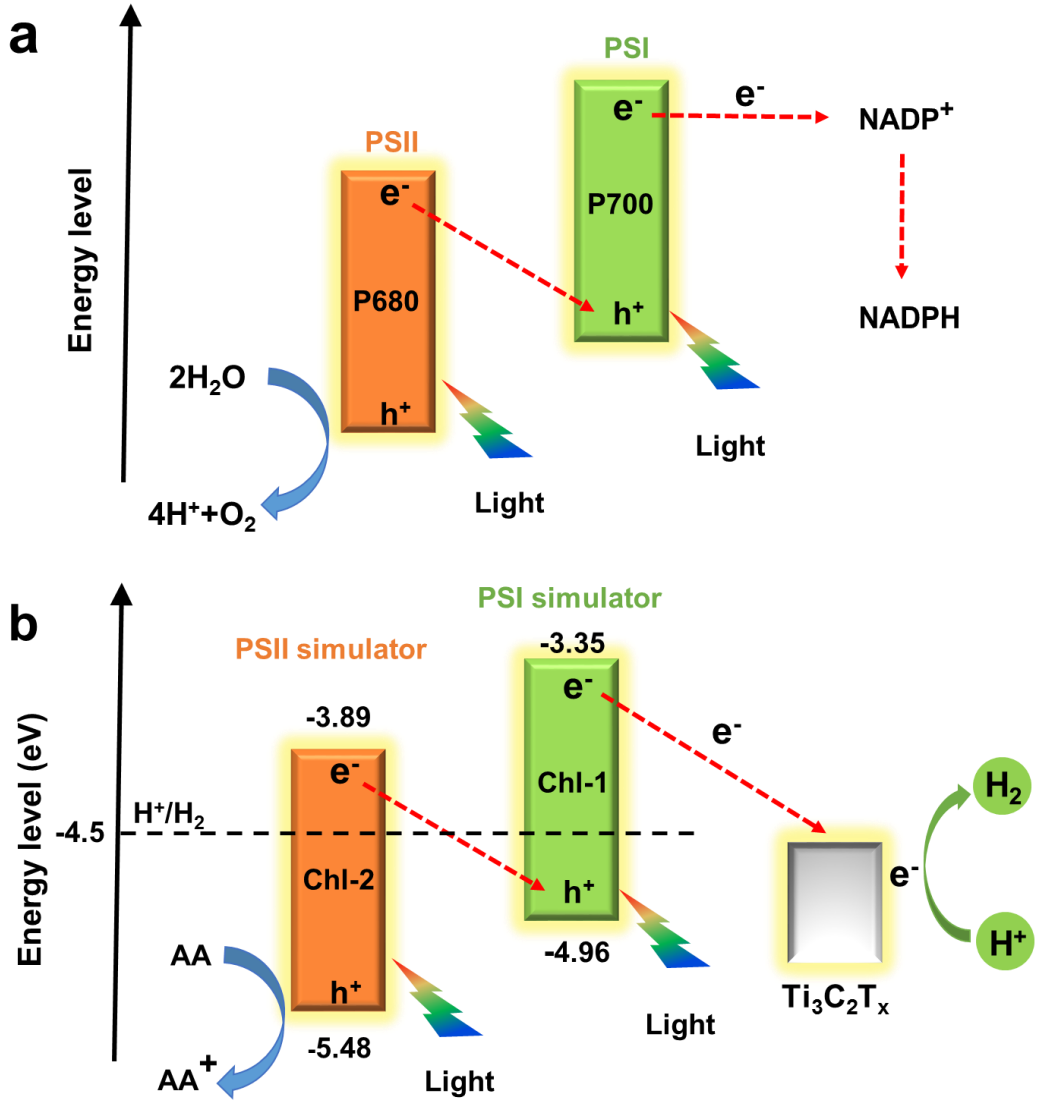

Fig. 7 (a) Schematic drawings of the photosynthetic natural Z-scheme and (b) schematic diagram of hydrogen production for Chl-1@Chl-2@$Ti_3C_2T_x$ composites under visible light irradiation.

Conclusion

In summary, Chl-1@Chl-2@$Ti_3C_2T_x$ organic heterojunction chlorophyll based noble metal-free photocatalysts was prepared by a simple alternative deposition process. In this novel photocatalyst structure, Chl-1 acts as a PSI simulator and Chl-2 acts as a PSII simulator to mimic the Z-scheme process of oxygenic photosynthesis. The best photocatalytic performance achieves 143 μmol/h/g_{cat} under visible light illumination ($\lambda >$ 420 nm), which was much higher than that of the control samples of either Chl-1@$Ti_3C_2T_x$ (20 μmol/h/g) or Chl-2@$Ti_3C_2T_x$ (15 μmol/h/g). This work established a new method to fabricate organic heterojunction photocatalysts with Z-Scheme architecture on the 2D nanosheets for potential high performance HER. Based on this work, we believe that not only chlorophyll derivatives but also other organic aggregate materials will also be applicable to this system. Therefore, the issues that were explored in this study can open new ways in the development of other organic aggregates materials systems for various applications. So that, this work will be more widely applied in HER in the future.

Experimental section

Synthesis of Chl and $Ti_3C_2T_x$ MXenes

Chl-1 and Chl-2 were prepared as previously reported.[33, 44] $Ti_3C_2T_x$ MXenes are obtained by etching Ti_3AlC_2 (Forsman, 98%) in 49% HF as follows. 49% HF (20 mL) was stirred at 300 rpm, and Ti_3AlC_2 (2 g) were slowly added at room temperature for 24 h. After that, the obtained solution was washed and centrifuged with deionized water

several times until neutral pH was reached, then the $Ti_3C_2T_x$ sediment was collected after discarding the supernatant. Finally, $Ti_3C_2T_x$ MXenes was dried in vacuum oven at 50 ℃ for 12 h.

Preparation of Chl-1@Chl-2@$Ti_3C_2T_x$ composites

$Ti_3C_2T_x$ (3 mg) and a certain amount of Chl-1 were dissolved in tetrahydrofuran (THF). The mass ratios between Chl-1 and $Ti_3C_2T_x$ were 0.5% (15 μg), 2% (60 μg), 4% (120 μg), or 8% (240 μg). The Chl-1@$Ti_3C_2T_x$ mixture was stirred at room temperature for 10 h until dry. Then, Chl-1@$Ti_3C_2T_x$ mixture and a certain amount of Chl-2 were dissolved in chlorobenzene. The mass ratios between Chl-2 and $Ti_3C_2T_x$ were 0.5% (15 μg), 2% (60 μg), 4% (120 μg), or 8% (240 μg). The Chl-1@Chl-2@$Ti_3C_2T_x$ mixture was stirred at room temperature for 48 h until dry.

Characterization

To characterize Chl-1, Chl-2, $Ti_3C_2T_x$, and the composites, an X-ray diffractometer (XRD, D8 Advance, Bruker) was operated at 40 kV and 200 mA with Cu Kα radiation (λ = 0.15406 nm). Scanning electron microscopy (SEM, SU8000, Hitachi) and high-resolution transmission electron microscopy (HRTEM, JEM-2200FS, JEOL) were used to observe the morphology of the samples. Fourier transform infrared spectroscopy (FT-IR, Vertex70, Bruker) was used to record the spectra of the samples in a range of 400 to 3100 cm^{-1}. Electronic absorption spectra of samples were measured with a UV-vis spectrometer (UV-3600, Shimadzu).

Photocatalytic activity measurements

Photocatalytic H_2 evolution was measured under a 300 W Xenon lamp (PLS-SXE

300, Beijing Perfectlight Technology): the light intensity was 100 mW/cm^2. A 6 mL photoreactor and a cut-off filter (usually $\lambda > 420$ nm) were used. Typically, 3 mg of as-prepared Chl-1@Chl-2@$Ti_3C_2T_x$ photocatalysts composite was added in aqueous 55 mM AA solution (3 mL). The mixture was sonicated for 5 min before light irradiation to fully disperse the composite. Argon was purged to remove oxygen in the solution and the reactor for 10 min. The reactants were continuously stirred under irradiation of visible-to-near infrared light ($\lambda > 420$ nm). The hydrogen production was measured after the 6 h by a gas chromatograph (SP-3420A, Beijing Beifen-Ruili Analytical Instrument) with a thermal conductivity detector. The average values were obtained by five independent experiments. The carrier gas was argon and the column contained 5 Å molecular sieves.

Photoelectrochemical activity test

EIS measurements in the range of 0.1 Hz to 100 kHz were carried out with an electrochemical workstation (Bio-Logic SAS) in a standard three-electrode system. The working electrode was prepared by ultrasonically dispersing the Chl-1@Chl-2@$Ti_3C_2T_x$ composite (10 mg) in a mixture of deionized water (250 μL), ethanol (250 μL) and Nafion solution (20 μL, Sigma-Aldrich, 5 wt%) for 5 min, then the dispersion (20 μL) was drop coated at room temperature onto an FTO square substrate (2 cm^2).[39] Ag/AgCl was used as the reference electrode and Pt plate was used as the counter electrode. The electrolyte was aqueous 0.5 M Na_2SO_4 solution containing AA (2 g/L). TPC response was measured in the same three-electrode system. A 300 W Xenon lamp with a cut-off filter ($\lambda > 420$ nm) was used as the light source. All measurements were conducted at room temperature.

Acknowledgements

This work was supported by the National Natural Science Foundation of China (No. 11974129 to X.-F. W.) and "the Fundamental Research Funds for the Central Universities, Jilin University" and Japan Society for the Promotion of Science (JSPS) KAKENHI Grant Number JP17H06436 (to H.T.).

Conflict of interest

The authors declare no conflict of interest.

Keywords: Z-scheme • chlorophyll • $Ti_3C_2T_x$ MXenes • organic heterojunction photocatalysts • hydrogen evolution reaction

References

[1] X. Lu, S. Xie, H. Yang, Y. Tong and H. Ji, *Chem. Soc. Rev.* **2014**, 43, 7581-7593.

[2] J. Ran, J. Zhang, J. Yu, M. Jaroniec and S. Z. Qiao, *Chem. Soc. Rev.* **2014**, 43, 7787-7812.

[3] Y. Tachibana, L. Vayssieres and J. R. Durrant, *Nat. Photonics* **2012**, 6, 511-518.

[4] E. Kabir, P. Kumar, S. Kumar, A. A. Adelodun and K.-H. Kim, *Renew. Sustain. Energy Rev.* **2018**, 82, 894-900.

[5] A. Kudo and Y. Miseki, *Chem. Soc. Rev.* **2009**, 38, 253-278.

[6] Y. Sun, X.-F. Wang, G. Chen, C.-H. Zhan, O. Kitao, H. Tamiaki and S.-i. Sasaki, *Int. J. Hydrogen Energy* **2017**, 42, 15731-15738.

[7] A. J. BARD, *J. Photochem.* **1979**, 10, 59-75.

[8] T. Mirkovic, E. E. Ostroumov, J. M. Anna, R. van Grondelle, Govindjee and G. D. Scholes, *Chem. Rev.* **2017**, 117, 249-293.

[9] S.-i. Sasaki, X.-F. Wang, T. Ikeuchi and H. Tamiaki, *J. Porphyrins Phthalocyanines* **2015**, 19, 517-526.

[10] S. Shoji, T. Ogawa, T. Hashishin, S. Ogasawara, H. Watanabe, H. Usami and H. Tamiaki, *Nano Lett.* **2016**, 16, 3650-3654.

[11] S. Duan, C. Dall'Agnese, G. Chen, X.-F. Wang, H. Tamiaki, Y. Yamamoto, T. Ikeuchi and S.-i. Sasaki, *ACS Energy Lett.* **2018**, 3, 1708-1712.

[12] N. Li, C. Dall'Agnese, W. Zhao, S. Duan, G. Chen, S.-i. Sasaki, H. Tamiaki, Y. Sanehira, T. Miyasaka and X.-F. Wang, *Mater. Chem. Front.* **2019**, 3, 2357-2362.

[13] B. Wang, L. Yang, C. Dall'Agnese, A. K. Jena, S.-i. Sasaki, T. Miyasaka, H. Tamiaki and X.-F. Wang, *Sol. RRL* **2020**, 7, 2000166.

[14] C. Zhang, W. Zhao, S.-i. Sasaki, H. Tamiaki and X.-F. Wang, *Electrochim. Acta* **2020**, 347, 136283.

[15] Y. Li, X. Chen, Y. Sun, X. Meng, Y. Dall'Agnese, G. Chen, C. Dall'Agnese, H. Ren, S. i. Sasaki, H. Tamiaki and X. F. Wang, *Adv. Mater. Interfaces* **2020**, 7, 1902080.

[16] Z. Pan, F. Cao, X. Hu and X. Ji, *J. Mater. Chem. A*, **2019**, 7, 8984-8992.

[17] S. Sun, Z. Xie, Y. Yan and S. Wu, *Chem. Eng. J.* **2019**, 366, 460-467.

[18] B. Anasori, M. R. Lukatskaya and Y. Gogotsi, *Nat. Rev. Mater.* **2017**, 2, 16098.

[19] L. Yang, C. Dall'Agnese, Y. Dall'Agnese, G. Chen, Y. Gao, Y. Sanehira, A. K. Jena, X. F. Wang, Y. Gogotsi and T. Miyasaka, *Adv. Funct. Mater.* **2019**, 29, 1905694.

[20] A. Agresti, A. Pazniak, S. Pescetelli, A. Di Vito, D. Rossi, A. Pecchia, M. Auf der Maur, A. Liedl, R. Larciprete, D. V. Kuznetsov, D. Saranin and A. Di Carlo, *Nat.*

Mater. **2019**, 18, 1228-1234.

[21] M. Han, X. Yin, H. Wu, Z. Hou, C. Song, X. Li, L. Zhang and L. Cheng, *ACS Appl. Mater. Interfaces* **2016**, 8, 21011-21019.

[22] X. Li, X. Yin, M. Han, C. Song, H. Xu, Z. Hou, L. Zhang and L. Cheng, *J. Mater. Chem. C* **2017**, 5, 4068-4074.

[23] Y. Ying, Y. Liu, X. Wang, Y. Mao, W. Cao, P. Hu and X. Peng, *ACS Appl. Mater. Interfaces* **2015**, 7, 1795-1803.

[24] Y. Sun, D. Jin, Y. Sun, X. Meng, Y. Gao, Y. Dall'Agnese, G. Chen and X.-F. Wang, *J. Mater. Chem. A* **2018**, 6, 9124-9131.

[25] M. Naguib, M. Kurtoglu, V. Presser, J. Lu, J. Niu, M. Heon, L. Hultman, Y. Gogotsi and M. W. Barsoum, *Adv. Mater.* **2011**, 23, 4248-4253.

[26] M. Alhabeb, K. Maleski, B. Anasori, P. Lelyukh, L. Clark, S. Sin and Y. Gogotsi, *Chem. Mater.* **2017**, 29, 7633-7644.

[27] H. Zhang, M. Li, J. Cao, Q. Tang, P. Kang, C. Zhu and M. Ma, *Ceram. Int.*, **2018**, 44, 19958-19962.

[28] M. Naguib, V. N. Mochalin, M. W. Barsoum and Y. Gogotsi, *Adv. Mater.* **2014**, 26, 992-1005.

[29] Y. Sun, Y. Sun, X. Meng, Y. Gao, Y. Dall'Agnese, G. Chen, C. Dall'Agnese and X.-F. Wang, *Catal. Sci. Tech.* **2019**, 9, 310-315.

[30] K. Xiong, P. Wang, G. Yang, Z. Liu, H. Zhang, S. Jin and X. Xu, *Sci. Rep.* **2017**, 7, 15095.

[31] Y. Li, X. Deng, J. Tian, Z. Liang and H. Cui, *Appl. Mater. Today* **2018**, 13, 217-

227.

[32] Y. Sun, X. Meng, Y. Dall'Agnese, C. Dall'Agnese, S. Duan, Y. Gao, G. Chen and X.-F. Wang, *Nano-Micro Lett.* **2019**, 11, 79.

[33] H. Tamiaki, M. Amakawa, Y. Shimono, R. Tanikaga, A. R. Hotzwarth and K. Schaffnel, *Photochem. Photobiol.* **1996**, 63, 92-99.

[34] M. Li, N. Li, W. Hu, G. Chen, S.-i. Sasaki, K. Sakai, T. Ikeuchi, T. Miyasaka, H. Tamiaki and X.-F. Wang, *ACS Appl. Energy Mater.* **2018**, 1, 9-16.

[35] Y. Li, S.-i. Sasaki, H. Tamiaki, C.-L. Liu, J. Song, W. Tian, E. Zheng, Y. Wei, G. Chen, X. Fu and X.-F. Wang, *J. Power Sources* **2015**, 297, 519-524.

[36] Q. Xue, H. Zhang, M. Zhu, Z. Pei, H. Li, Z. Wang, Y. Huang, Y. Huang, Q. Deng, J. Zhou, S. Du, Q. Huang and C. Zhi, *Adv. Mater.* **2017**, 29, 1604847.

[37] Y. Lu, M. Yao, A. Zhou, Q. Hu and L. Wang, *J. Nanomater*. **2017**, 5, 1978764.

[38] M. Li, S.-i. Sasaki, Y. Sanehira, T. Miyasaka, H. Tamiaki, T. Ikeuchi, G. Chen and X.-F. Wang, *J. Photochem. Photobiol., A* **2018**, 353, 639-644.

[39] T. Su, R. Peng, Z. D. Hood, M. Naguib, I. N. Ivanov, J. K. Keum, Z. Qin, Z. Guo and Z. Wu, *ChemSusChem* **2018**, 11, 688-699.

[40] T. Kothe, N. Plumere, A. Badura, M. M. Nowaczyk, D. A. Guschin, M. Rogner and W. Schuhmann, *Angew. Chem. Int. Ed.* **2013**, 52, 14233-14236.

[41] V. Hartmann, T. Kothe, S. Poller, E. El-Mohsnawy, M. M. Nowaczyk, N. Plumere, W. Schuhmann and M. Rogner, *Chem. Chem. Phys.* **2014**, 16, 11936-11941.

[42] K. Brettel and W. Leibl, *Biochim. Biophys. Acta* **2001**, 1507, 100-114.

[43] Y. Kim, D. Shin, W. J. Chang, H. L. Jang, C. W. Lee, H.-E. Lee and K. T. Nam,

Adv. Funct. Mater. **2015**, 25, 2369-2377.

[44] S.-i. Sasaki, M. Yoshizato, M. Kunieda and H. Tamiaki, *Eur. J. Org. Chem.* **2010**, 27, 5287-5291.

TOC figure